

Theoretical verification of intermolecular hydrogen bond induced thermally activated delayed fluorescence in SOBF-OMe

Mu-Zhen Li(李慕臻), Fei-Yan Li(李飞雁), Qun Zhang(张群), Kai Zhang(张凯), Yu-Zhi Song(宋玉志), Jian-Zhong Fan(范建忠), Chuan-Kui Wang(王传奎), and Li-Li Lin(蔺丽丽)

Citation: Chin. Phys. B, 2021, 30 (**12**): 123302. DOI: 10.1088/1674-1056/ac1b91
Journal homepage: http://cpb.iphy.ac.cn; http://iopscience.iop.org/cpb

What follows is a list of articles you may be interested in

Effects of temperature and pressure on OH laser-induced fluorescence exciting A-X (1,0) transition at high pressures

Xiaobo Tu(涂晓波), Linsen Wang(王林森), Xinhua Qi(齐新华), Bo Yan(闫博), Jinhe Mu(母金河), Shuang Chen(陈爽)

Chin. Phys. B, 2020, 29 (**9**): 093301. DOI: 10.1088/1674-1056/aba5ff

Energy transfer, luminescence properties, and thermal stability of color tunable barium pyrophosphate phosphors

Meng-Jiao Xu(徐梦姣), Su-Xia Li(李素霞), Chen-Chen Ji(季辰辰), Wan-Xia Luo(雒晚霞), Lu-Xiang Wang(王鲁香)

Chin. Phys. B, 2020, 29 (**6**): 063301. DOI: 10.1088/1674-1056/ab821a

Exploring photocurrent output from donor/acceptor bulk-heterojunctions by monitoring exciton quenching

Wang Xin-Ping, He Zhi-Qun, Liang Chun-Jun, Qiu Hai-An, Jing Xi-Ping

Chin. Phys. B, 2015, 24 (**6**): 063301. DOI: 10.1088/1674-1056/24/6/063301

Fine-tuning the thicknesses of organic layers to realize high-efficiency and long-lifetime blue organic light-emitting diodes

Yu Jian-Ning, Zhang Min-Yan, Li Chong, Shang Yu-Zhu, Lü Yan-Fang, Wei Bin, Huang Wei

Chin. Phys. B, 2012, 21 (**8**): 083303. DOI: 10.1088/1674-1056/21/8/083303

Theoretical verification of intermolecular hydrogen bond induced thermally activated delayed fluorescence in SOBF-OMe*

Mu-Zhen Li(李慕臻), Fei-Yan Li(李飞雁), Qun Zhang(张群), Kai Zhang(张凯), Yu-Zhi Song(宋玉志), Jian-Zhong Fan(范建忠), Chuan-Kui Wang(王传奎)†, and Li-Li Lin(蔺丽丽)‡

Shandong Key Laboratory of Medical Physics and Image Processing & Shandong Provincial Engineering and Technical Center of Light Manipulations, School of Physics and Electronics, Shandong Normal University, Jinan 250358, China

(Received 30 June 2021; revised manuscript received 28 July 2021; accepted manuscript online 7 August 2021)

Thermally activated delayed fluorescence (TADF) molecules have attracted great attention as high efficient luminescent materials. Most of TADF molecules possess small energy gap between the first singlet excited state (S_1) and the first triplet excited state (T_1) to favor the up-conversion from T_1 to S_1. In this paper, a new TADF generation mechanism is revealed based on theoretical simulation. By systematic study of the light-emitting properties of SOBF-OMe in both toluene and in aggregation state, we find that the single SOBF-OMe could not realize TADF emission due to large energy gap as well as small up-conversion rates between S_1 and T_1. Through analysis of dimers, we find that dimers with intermolecular hydrogen bond (H-bond) are responsible for the generation of TADF, since smaller energy gap between S_1 and T_1 is found and the emission wavelength is in good agreement with experimental counterpart. The emission properties of SOBF-H are also studied for comparison, which reflect the important role of H-bond. Our theoretical results agree ith experimental results well and confirm the mechanism of H-bond induced TADF.

Keywords: organic light-emitting diodes, thermally activated delayed fluorescence, intermolecular hydrogen bond, decay rates

PACS: 33.50.–j, 33.50.Dq, 33.50.Hv **DOI:** 10.1088/1674-1056/ac1b91

1. Introduction

Compared with the liquid crystal display (LCD), organic light-emitting diodes (OLEDs) display, which are thinner provide better image quality and contrast.[1] On the basis of the spin-statistics, the ratio of singlet excitons produced in organic electroluminescent materials is one-quarter, and the ratio of triplet excitons is three-quarters.[2,3] For conventional fluorescent OLEDs, the internal quantum efficiency (IQE) is much lower than other OLDEs due to the unavailability of triplet excitons. Since OLEDs with thermally activated delayed fluorescence (TADF) emitters which can obtain luminous singlet and triplet excited states through an effective reverse intersystem crossover (RISC) process were reported to achieve nearly 100% exciton efficiency, TADF materials have attracted widespread attention.[4–6] Although the current application of TADF-OLEDs is still far inferior to phosphorescent OLEDs, due to the high cost and limited resources of phosphorescent materials, TADF-OLEDs still has a lot of room for development as next-generation electroluminescent material.[7–11] For TADF molecules, the most common structure is the donor–acceptor (D–A) or D–A–D configuration. The separation of highest occupied molecular orbital (HOMO) and the lowest unoccupied molecular orbital (LUMO) relies on such twisted, spiral or bulky connection structures, which will effectively reduce the overlap between HOMO and LUMO, and thus reduce the energy gap between S_1 and T_1 (ΔE_{ST}).[12–14] There is also TADF produced in the host–guest doped system.[15–17] The characteristics of the host can directly affect the energy of the charge transfer (CT) state and the the ΔE_{ST} of the singlet state and the triplet state.[18] As host usually has a large energy gap, the vibration of singlet excitons on the TADF guest are generally well restricted.[19] Recent studies have found that the production of TADF can be assisted by intramolecular or intermolecular hydrogen bonds,[20,21] which indicates that intra- or intermolecular interactions can also promote the formation of TADF, while lack of theoretical verification made it difficult to be understood. Therefore, theoretical studies of the photophysical properties of TADF molecules with intra- or intermolecular hydrogen bonds will contribute to the understanding of the TADF luminescence mechanism. In this paper, we focus on 4-(4-((4-methoxyphenyl) sulfonyl) phenyl) dibenzo[b,d]furan (SOBF-OMe) and 4-(4-(phenylsulfonyl)phenyl)dibenzo[b,d]furan (SOBF-H) (as shown in Fig. 1(a), Fig. S1(a)) reported by Chi's group.[22] Therein, the TADF is observed for the SOBF-OMe in crystalline state, while no TADF is observed for it in solvent or for SOBF-H in crystalline state. It is deduced that the TADF for SOBF-OMe is generated through intermolecular hydro-

*Project supported by the National Natural Science Foundation of China (Grant Nos. 11974216, 11874242, 21933002, and 11904210), the Natural Science Foundation of Shandong Province, China (Grant No. ZR2019MA056), the Taishan Scholar Project of Shandong Province, China, and the Project funded by China Postdoctoral Science Foundation (Grant No. 2018M642689).

†Corresponding author. E-mail: ckwang@sdnu.edu.cn

‡Corresponding author. E-mail: linll@sdnu.edu.cn

© 2021 Chinese Physical Society and IOP Publishing Ltd

gen bond. To verify the generation mechanism of TADF in SOBF-OMe, adopting the quantum mechanics and molecular mechanics (QM/MM) method to simulated the light-emitting property of two molecules in crystalline state.[23] Both monomers and dimers are used as models to exploring the origin of TADF. Our results will help to better understand the TADF phenomenon in SOBF-OME crystals, and expand the luminescence mechanism of TADF molecules, thus promoting the development of new multifunctional luminescent TADF molecules.

2. Theoretical methods

In this work, density functional theory (DFT) was used to optimize the ground state (S_0). We used the DFT method to optimize the ground state structures of molecules SOBF-OMe and SOBF-H. In addition, the excited state properties of TADF molecules directly determine the luminescence properties, the time-dependent density functional theory (TD-DFT) to optimize the excited states. The frequency calculation of the optimized structure confirms the stability of the obtained geometric structure. In order to simulate the solvent of toluene, we used the polarizable continuum model (PCM), which can accurately predict the effect of solvents on TADF molecules.[24–26] The combination of quantum mechanics and molecular mechanics (QM/MM) is used to simulate the properties of molecules in the aggregation state which has been proven reliable.[27–30] Meanwhile, we use a two-layer ONIOM model (as shown in Fig. 1(b), and Fig. S1(b)) with the center as the high layer and the surrounding as the low layer, where the high layer is calculated using the QM method and the low layer is calculated using the MM method. Further more, we use the universal force field (UFF) and TD-DFT methods for the components of MM and QM, respectively.[31–33] Three functionals (TPSSH, B3LYP, BMK) and two range separation functionals (CAM-B3LYP, ωB97XD) are tested and the 6-31G(d) basis set is used (as listed in Table 1). For dimers, the above functional combined with the empirical dispersion correlation (GD3) is calculated.[34] The calculated emission wavelengths of SOBF-OMe and SOBF-H in the solid phase calculated with the B3LYP functional are found to be similar to the experimental results. Therefore, the subsequent calculations were carried out at the level of B3LYP/6-31G(d). Perform the above calculation process in the Gaussian 16 program.[35]

Table 1. Emission wavelengths calculated value with different functionals for SOBF-H and SOBF-OMe in aggregation state (in unit nm).

	SOBF-H	SOBF-OMe
TPSSH	389	457
B3LYP	357	408
BMK	305	311
CAM-B3LYP	299	305
ωB97XD	297	303
Exp.	350	380

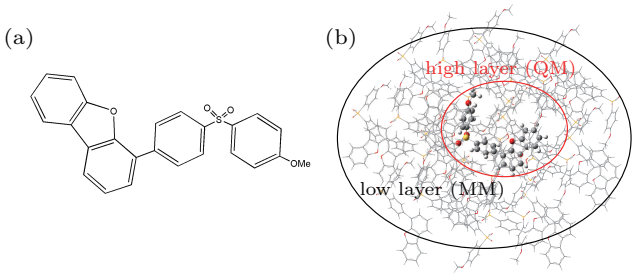


Fig. 1. (a) Chemical structures of SOBF-OMe. (b) ONIOM model of SOBF-OMe: the center molecule is the high layer, and the others molecules are the low layer.

For the radiative decay rate, the Einstein's spontaneous emission formula is

$$k_{\mathrm{r}} = \frac{f\Delta E_{\mathrm{fi}}^2}{1.499\ \mathrm{cm}^{-2}\cdot\mathrm{s}}, \tag{1}$$

where f represents the oscillator strength and ΔE_{fi} the unit is the wave number (cm^{-1}) is the energy difference between S_1 and S_0.[36]

Similarly, the intersystem crossing (ISC) rate can be written as

$$k_{\mathrm{ISC}} = \frac{1}{\hbar^2}\left\langle \Phi_{\mathrm{f}}\left|\widehat{H}^{\mathrm{so}}\right|\Phi_i\right\rangle \int_{-\infty}^{\infty} \mathrm{d}t\left[\mathrm{e}^{\mathrm{i}\omega_{\mathrm{tf}}} Z_{\mathrm{i}}^{-1}\rho_{\mathrm{ISC}}(t,T)\right], \tag{2}$$

where Z_{i} stands for partition function and $\rho_{\mathrm{ISC}}(t,T)$ represents the thermal vibration correlation function. We also use formula (2) to calculate the reverse intersystem crossing (RISC) rate. The ISC rate and RISC rates are calculated by MOMAP (Molecular Materials Property Prediction Package).[37–39]

The independent gradient model (IGM) is used to measure interactions between molecules in the aggregated state due to its accurate visualization.[40] The equations are as follows:

$$\delta g(r) = g^{\mathrm{IGM}}(r) - g(r), \tag{3}$$

$$g(r) = \left|\sum_i \nabla\rho_i(r)\right|, \tag{4}$$

$$g^{\mathrm{IGM}}(r) = \left|\sum_i \mathrm{abs}\left[\nabla\rho_i(r)\right]\right|, \tag{5}$$

where i stands for the atomic ordinal number and $\nabla\rho$ represents the gradient vector; abs($\nabla\rho$) is that every component of $\nabla\rho$ vector takes the absolute value.

Besides, energy decomposition analysis based on the molecular force field is performed to characterize various weak interactions.[41] Most molecular force fields use the form of pair potential to calculate the electrostatic, exchange repulsion and dispersion attraction parts of the non-bonded interaction between atoms.[42] The relevant formula applied is as follows:

$$E_{\mathrm{AB}}^{\mathrm{ele}} = \frac{q_{\mathrm{A}}q_{\mathrm{B}}}{r_{\mathrm{AB}}}, \tag{6}$$

$$E_{\mathrm{AB}}^{\mathrm{vdW}} = E_{\mathrm{AB}}^{\mathrm{rep}} + E_{\mathrm{AB}}^{\mathrm{disp}}, \tag{7}$$

$$E_{\mathrm{AB}}^{\mathrm{rep}} = \varepsilon\left(\frac{R_{\mathrm{AB}}^0}{r_{\mathrm{AB}}}\right)^{12}, \tag{8}$$

$$E_{AB}^{disp} = -2\varepsilon_{AB}\left(\frac{R_{AB}^{0}}{r_{AB}}\right)^{6}, \quad (9)$$

where A and B are the atomic labels, q stands for the atomic charge, r is the distance between atoms, ε is the depth of the van der Waals potential well, and R^0 is the non-bonded distance between atoms.

3. Results and discussion

The light-emitting properties of monomers are studied first to check its possible contribution for TADF. Based on the initial structure in crystal, we optimized the geometry of the molecule in the ground state (S_0), the first singlet excited state (S_1), and the triplet excited state (T_N) in the toluene and aggregation state respectively. At the same time, the root-mean-square displacement (RMSD) method in Multiwfn is combined to show the structural differences between the different states (ground and excited). Moreover, due to different restriction conditions, there is a difference between the optimized molecular geometry in toluene and the optimized molecular geometry in the aggregate state as shown in Fig. 2. It can also be found that there are significant differences between the dibenzofuran and benzene rings. The RMSD values in toluene is much larger than that in aggregation state, indicating that intermolecular interaction could limit the motion of the units in aggregation when they are excited. For TADF molecules, the up-conversion process is closely related to the energy difference between S_1 and T_1 (ΔE_{ST}).

Therefore, the adiabatic excitation energies for SOBF-OMe in toluene and aggregation state are calculated respectively (see Fig. 3). Further more, the calculated ΔE_{ST} in toluene and aggregation state is 1.22 eV and 1.08 eV respectively, indicating that ΔE_{ST} can be reduced by intermolecular interaction. It also indicates that it is difficult for them to realize up-conversion from T_1 to S_1. In addition, the comparison of excited state energy levels in toluene shows that T_2, T_3, T_4, and T_5 are not only lower than S_1 but also close to S_1 in terms of energy. It is suggested that not only T_1 but also T_2, T_3, T_4, and T_5 may participate in ISC and RISC processes. In the aggregation state (as shown in Fig. 3(b)), we find that the energy of S_1 is 0.01 eV lower than that of T_5. The higher triplet states that close to S_1 in energy may favor the ISC process, which would be disadvantage to the emission. By comparing the energy structures of molecules in toluene and aggregation state, it is concluded that the interaction between molecules in aggregation state will affect the energy level structure and the ISC and RISC processes of the excited state.

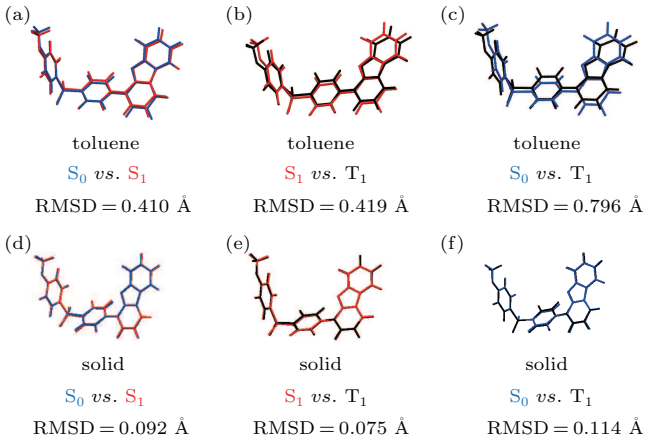


Fig. 2. Geometry difference between S (blue), S_1 (red), and T_1 (black) in toluene [(a), (b), (c)] and in aggregation state [(d), (e), (f)].

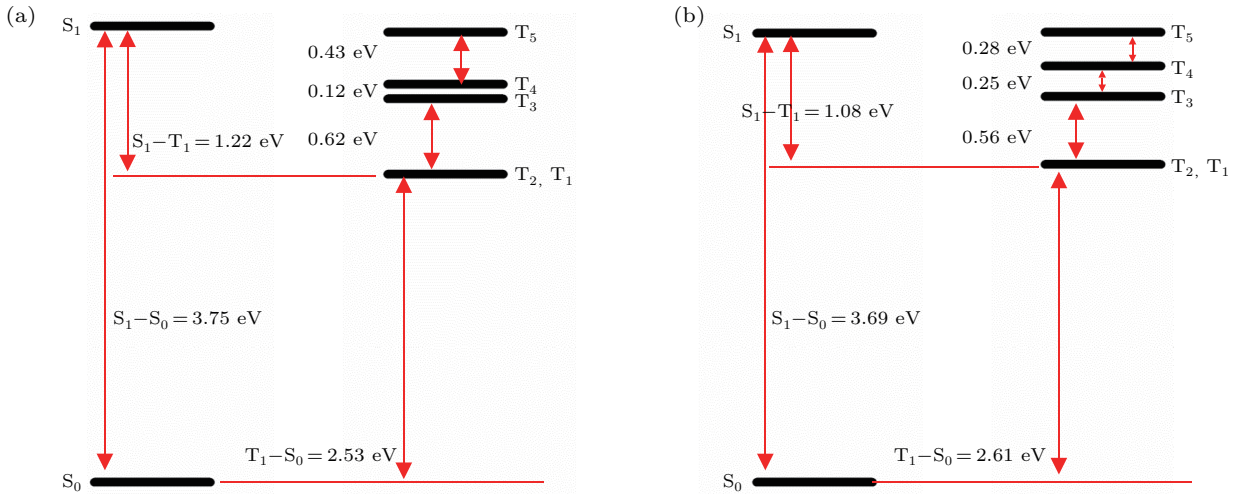


Fig. 3. Energy levels for SOBF-OMe in toluene (a) and in aggregation state (b) respectively.

In order to further elucidate the excited state transition properties of SOBF-OMe, we analyzed the natural transition orbital (NTO) and the corresponding transition properties of SOBF-OMe (as shown in Fig. 4). Through the transformation of molecular orbital, we qualitatively describe the mechanism of electron excitation.[43,44] The local excited (LE) state (with the LE components are 75%–100%) predicts a large orbital overlap. While the charge transfer (CT) state with strong charge transfer properties (with the LE components are 0%–40%) leads to a small S_1–T_1 energy gap due to significant orbital separation. The hybridized local and charge transfer (HLCT) excited state (with the LE components are 40%–75%) is the LE and CT are mixed, with both

LE and CT properties.[45–47] Figures 4(a) and 4(b) show the NTOs of S_1 and T_N obtained by Multiwfn in toluene and aggregated state. We can intuitively see that S_1 is a typical hybridized local and charge-transfer excited state, there is significant overlap in the conjugation chain between electron and hole, whether it is in toluene or in aggregation state. However, the transitions of the triplet state are mainly distributed in the benzene ring and the dibenzofuran group, except for the T_3 state. The aggregation state has little effect on the transition properties, compared with that in toluene.

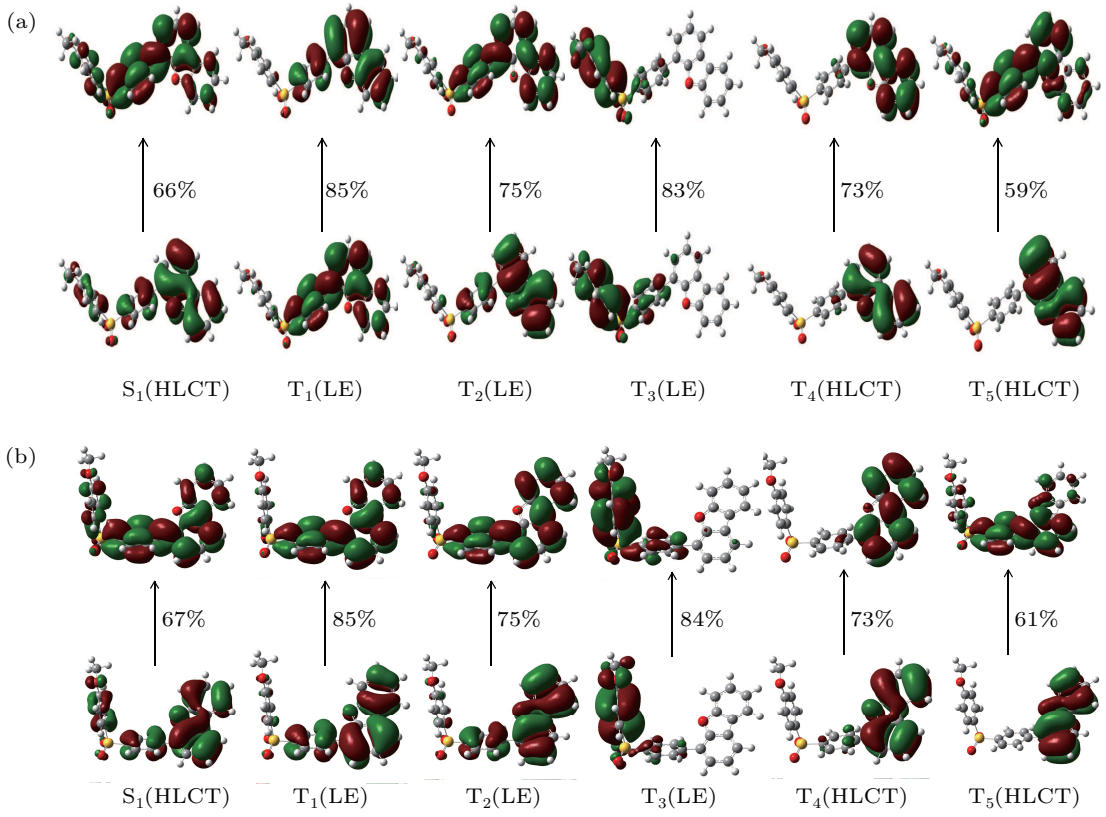


Fig. 4. NTOs for S_1 and T_N sates of SOBF-OMe for monomer in toluene (a) and aggregation state (b) respectively (isovalue is 0.02).

Based on the energy levels of excited states, the ISC processes from S_1 to T_N should be quite possible in both toluene and aggregation state. The ISC process is not only related to ΔE_{ST}, but also to the spin–orbit coupling (SOC) constant. Table 2 lists the SOC values in toluene and aggregation state, calculated with the quadratic response function method in Dalton package.[48] In aggregation state, the ISC rate between S_1 and T_1 (2.03×10^7 s^{-1}) is greater than that in toluene (8.89×10^5 s^{-1}), may be induced by the small SOC constant in toluene. The RISC rates are also calculated based on the SOC values calculated in triplet states. The values are all quite small due to the large energy gap between them. Although the RISC values from T_5 to S_1 is comparable to the ISC value, it is meaningless since little excitons would distribute on T_5. It proves that it is impossible for the RISC process to happen in the single molecule. Moreover, the radiation decay rate in toluene is 4.43×10^8 s^{-1}, which is larger than that in aggregate state (5.23×10^7 s^{-1}). The main reason should be that the energy difference between S_1 and S_0 in aggregate state (3.69 eV) is smaller than that of toluene (3.75 eV). The non-radiation rate in aggregation (1.06×10^{11} s^{-1}) is a little lower than that in toluene (2.92×10^{11} s^{-1}), which may be induced by the confinement of the surroundings.

Table 2. Spin–orbit coupling (SOC) constant, intersystem crossing (ISC) rate, and reverse intersystem crossing (RISC) rate between S_1 and T_N.

	State	SOC[a] (cm^{-1})	k_{ISC} (s^{-1})	SOC[b] (cm^{-1})	k_{RISC} (s^{-1})
Toluene	S_1–T_1	0.143	8.89×10^5	0.077	4.87×10^{-6}
	S_1–T_2	0.054	1.27×10^5	0.031	3.06×10^{-6}
	S_1–T_3	0.630	4.96×10^7	0.205	1.24×10^{-4}
	S_1–T_4	0.816	1.66×10^7	0.864	7.31×10^{-1}
	S_1–T_5	0.086	1.17×10^2	0.250	1.11×10^3
Aggregation	S_1–T_1	0.731	2.03×10^7	0.224	1.45×10^{-5}
	S_1–T_2	0.667	1.02×10^8	0.401	3.43×10^{-3}
	S_1–T_3	0.633	3.83×10^7	0.506	9.41×10^{-2}
	S_1–T_4	2.010	7.03×10^8	0.639	3.12×10^3
	S_1–T_5	1.360	1.28×10^6	0.286	1.63×10^6

Notes: [a]Calculated based on the optimized geometry of S_1.
[b]Calculated based on the optimized geometry of T_N.

The photophysical properties for SOBF-H are also studied in both toluenet and aggregation state. From the energy level of the excited state (see Fig. S2), we find that the excited state energy level of SOBF-H is similar to the SOBF-OMe

molecule. In aggregation state, the energy gap between S_1 and T_1 (1.18 eV) is slightly larger than that for SOBF-OMe (1.08 eV). The transition orbitals change slightly between the two molecules (see Fig. S3), where the LE component for SOBF-H decreases in S_1 and increases in T_1. In addition, the SOC constant between S_1 and T_5 in aggregate state is decreased to (0.368 cm^{-1}) and the ISC rate is increased to (4.30×10^7 s^{-1}) (see Table S1). The RISC rate between S_1 and T_5 of SOBF-H (4.44×10^1 s^{-1}) is so small, it is difficult to produce thermally activated delayed fluorescence.

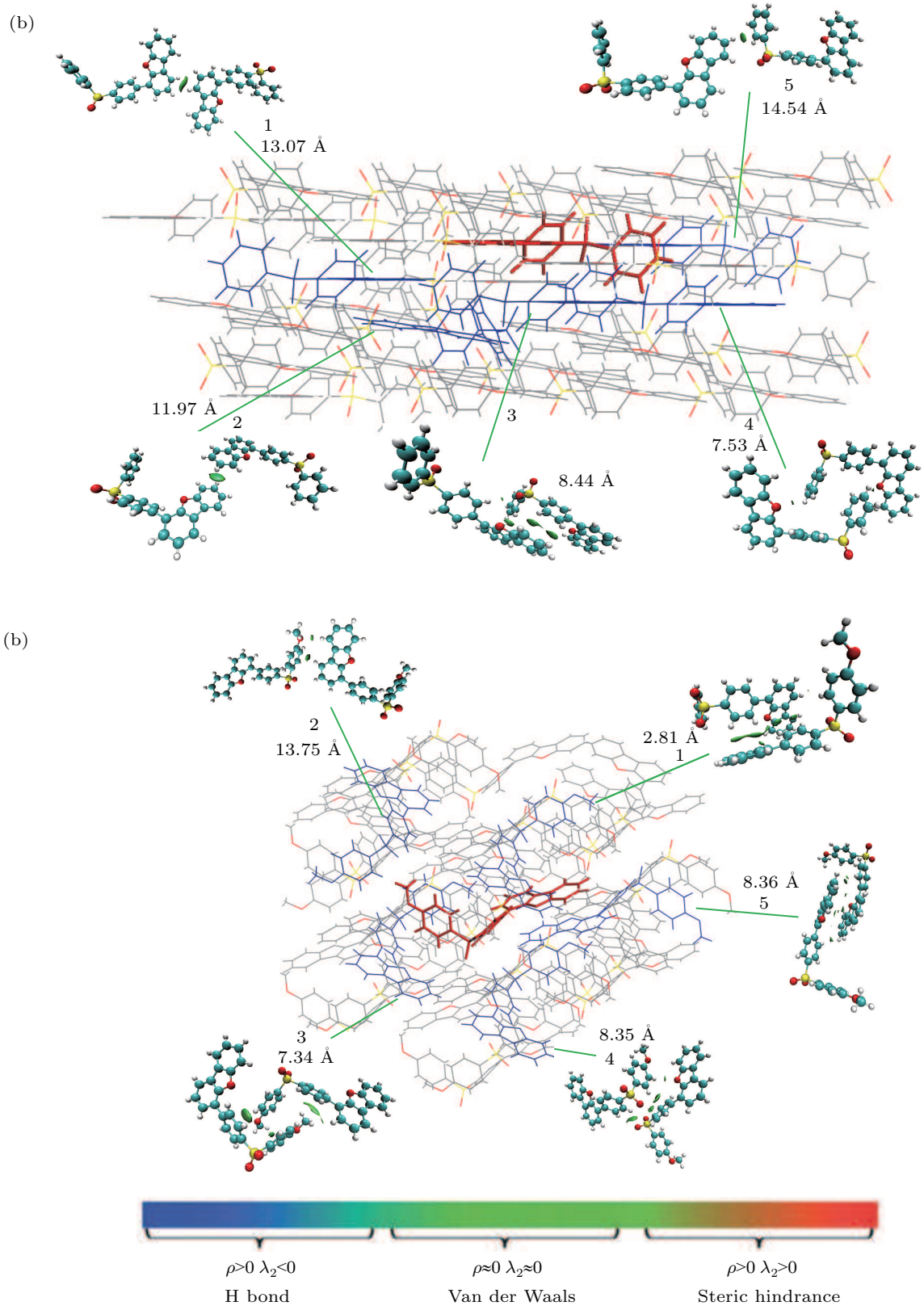


Fig. 5. Intermolecular interactions for several dimers described [SOBF-H (a) and SOBF-OMe (b)] through the IGM method.

In experiment, TADF was found for the SOBF-OMe in aggregation. Our calculation results of single molecules indicates that TADF could not be contributed by single molecules. Thus dimers which may contribute to TADF emission are studied. Based on the crystal structure of SOBF-H and SOBF-OMe, several dimers are studied, and the interaction between molecules was analyzed by the IGM method (see Fig. 5). Based on the energy decomposition of the AMBER force field, the interaction energy between neighboring molecules is shown in Table 3. For SOBF-OMe it can be seen that the intermolecular interaction of dimer-2 and dimer-4 is weaker, and the intermolecular interaction of dimer-1 is the strongest. Through further analysis, it is found that the dispersion between the two molecules dominates the intermolecular interaction. In addition, there is a π–π interaction in dimer-5, it is mainly the π–π interaction between dibenzofuran groups. In the same way, π–π interaction also exists in dimer-3, and the π–π stacking exists in the donor benzene ring. For SOBF-H the intermolecular interaction of dimer-1 and dimer-2 is weak. Through further analysis, we find that the dispersion between the two molecules dominates the intermolecular interaction. Using IGM analysis, it is found that SOBF-OMe dimer-2 and dimer-4 have obvious intermolecular hydrogen bond interactions. It is also found that dimer-3 and dimer-5 have significant π–π interraction. Then several pairs of dimers for SOBF-H and SOBF-OMe are optimized with the QM/MM model. The emission wavelengths and the S_1–T_1 energy gap for all the dimers are shown in Table 4. It can be seen that the calculated emission wavelengths of dimer-2 and dimer-4 for SOBF-OMe consistent with the experimental results of TADF. In addition, the ΔE_{ST} of S_1 and T_1 in dimer-2 is also much smaller than other dimers, which also predicts the possible up-conversion from triplest states to S_1. The NTOs of SOBF-H and SOBF-OMe dimer are also analyzed (see Fig. S4). It is found that both two dimers of SOBF-H have delocalized NTOs with electron distributed on both two molecules and significant overlap can be found for transition orbitals. However, the NTOs for dimers except for dimer-5 of SOBF-OMe indicate that electrons transit from one molecule to the other when they are excited. Although dimer-5 has strong π–π interaction, it is meaningless to the TADF emission. It favors the emission of phosphorescence. For the energy diagram of excited states, we can find that there are several states lying between S_1 and T_1, which may favor the ISC process and the emission of phosphorescence (see Figs. S5 and S6). The calculated wavelength of T_1 for all the dimers is also in consistent with the experimental result, which further illustrates that dimers except those with H-bond may favor the phosphorescence emission (see Table S2). Therefore, we believe that the intermolecular H-bond could induce smaller S_1–T_1 energy gap, thus the TADF could be generated. Dimers with π–π interaction would favor the phosphorescence emission.

Table 3. Intermolecular interaction energy including electronic, repulsion, and dispersion interactions in several dimers studied.

Compounds	System	Electrostatic (kJ/mol)	Repulsive (kJ/mol)	Dispersion (kJ/mol)	Total (kJ/mol)
SOBF-H	dimer-1	0.08	4.51	−13.10	−8.51
	dimer-2	−1.01	8.93	−19.59	−11.67
SOBF-OMe	dimer-1	−2.92	19.90	−70.23	−53.25
	dimer-2	−3.82	7.55	−23.29	−19.55
	dimer-3	15.91	31.70	−98.76	−51.15
	dimer-4	−24.25	66.54	−81.15	−38.86
	dimer-5	1.30	27.87	−80.50	−51.33

Table 4. Calculated fluorescence wavelength, ΔE_{ST} and oscillator strength of SOBF-OMe and SOBF-H for dimer based on their single crystal structures using TD-DFT method.

	SOBF-H		SOBF-OMe				
	dimer-1	dimer-2	dimer-1	dimer-2	dimer-3	dimer-4	dimer-5
Wave (nm)	361	364	393	461	373	440	373
ΔE_{ST} (eV)	1.14	1.08	0.91	0.52	1.08	0.64	0.99
$f(S_1-S_0)$	0.1708	0.0565	0.0010	0.0001	0.0981	0.0004	0.0060
Exp.	350				476		

4. Conclusion

The excited state properties and decay rates of SOBF-OMe in toluene and aggregation state are studied respectively. The results show that the intermolecular interaction could limit the geometric change of molecules when they are excited in aggregation state. The energy gaps between S_1 and T_1 are reduced to some extent, while the transition properties have little changed. Theoretical simulation of the single molecular emission in toluene and in aggregation state agrees well the prompt fluorescence and phosphorescence. It is also indicated that TADF could not be generated by single SOBF-OMe molecules but dimers with intermolecular H-bond in crystal. In addition, emission properties of SOBF-H are also investigated for comparison, which shows that dimers without intermolecular H-bond are unable to generate TADF. Our calculation results confirms experimental results that TADF could be induced by dimers with intermolecular H-bond, although that single molecules with large S_1–T_1 energy gap have no contri-

bution to it. The results would favor the development of new type light-emitting molecules with TADF emission.

References

[1] Wong M Y and Colman E Z 2017 *Adv. Mater.* **29** 1605444
[2] Masui K, Nakanotani H and Adachi C 2013 *Org. Electron.* **14** 2721
[3] Baldo M A, O'brien D F, You Y, Shoustikov A, Sibley S, Thompson M E and Forrest S R 1998 *Nature* **395** 151
[4] Tang C W and Vanslyke S A 1987 *App. Phys. Lett.* **51** 913
[5] Lv L L, Yuan K, Si C D, Zuo G F and Wang Y C 2020 *Org. Electron.* **81** 105667
[6] Hu T P, Tu Z Y, Han G C and Yi Y P 2021 *J. Phys. Chem. C* **125** 1249
[7] Lee C W and Lee J Y 2013 *Adv. Mater.* **25** 5450
[8] Kim S Y, Jeong W I, Mayr C, Park Y S, Kim K H, Lee J H, Moon C K, Brütting W and Kim J J 2013 *Adv. Funct. Mater.* **23** 3896
[9] Gan L, Gao K, Cai X, Chen D C and Su S J 2018 *J. Phys. Chem. Lett.* **9** 4725
[10] Yu Y J, Wang X Q, Liu J F, Jiang Z Q and Liao L S 2021 *Science* **24** 102123
[11] Nakanotani H, Tsuchiya Y and Adachi C 2021 *Chem. Lett.* **50** 938
[12] Tao Y, Yuan K, Chen T, Xu P, Li H H, Chen R F, Zheng C, Zhang L and Huang W 2014 *Adv. Mater.* **26** 7931
[13] Yao L, Zhang S T, Wang R, Li W J, Shen F Z, Yang B and Ma Y G 2014 *Angew. Chem. Int. Ed. Engl.* **53** 2119
[14] Ansari R, Shao W H, Yoon S J, Kim J and Kieffer J 2021 *ACS Appl. Mater. Inter.* **13** 28529
[15] Zhang X Q, Fuentes-Hernandez C, Zhang Y D, Cooper M W, Barlow S, Marder S R and Kippelen B 2018 *J. Appl. Phys.* **124** 055501
[16] Dos Santos P L, Ward J S, Bryce M R and Monkman A P 2016 *J. Phys. Chem. Lett.* **7** 3341
[17] Lei Y X, Yang J F, Dai W B, Lan Y S, Yang J H, Zheng X Y, Shi J B, Tong B, Cai Z X and Dong Y P 2021 *Chem. Sci.* **12** 6518
[18] Stavrou K, Franca L G and Monkman A P 2020 *ACS Appl. Electron. Mater.* **2** 2868
[19] Hauenstein C, Gottardi S, Bobbert P A, Coehoorn R and van Eersel H 2020 *J. Appl. Phys.* **128** 075501
[20] Xie Z L, Huang Q Y, Yu T, Wang L Y, Mao Z, Li W L, Yang Z, Zhang Y, Liu S W, Xu J R, Chi Z G and Aldred M P 2017 *Adv. Funct. Mater.* **27** 1703918
[21] Shi Y Z, Wang K, Tsuchiya Y, Liu W, Komino T, Fan X C, Sun D M, Dai G L, Chen J X, Zhang M, Zheng C J, Xiong S Y, Ou X M, Yu J, Jie J S, Lee C S, Adachi C and Zhang X H 2020 *Mater. Horiz.* **7** 2734
[22] Chen J R, Yu T, Ubba E, Xie Z L, Yang Z Y, Zhang Y, Liu S W, Xu J R, Aldred M P and Chi Z G 2019 *Adv. Opt. Mater.* **7** 1801593
[23] Wang B, Wang X J, Wang W L and Liu F Y 2016 *J. Phys. Chem. C* **120** 21850
[24] Lin L L, Wang Z J, Fan J Z and Wang C K 2017 *Org. Electron.* **41** 17
[25] Fan J Z, Lin L L and Wang C K 2016 *Chem. Phys. Lett.* **652** 16
[26] Fan D, Yi Y P, Li Z D, Liu W J, Peng Q and Shuai Z G 2015 *J. Phys. Chem. A* **119** 5233
[27] Fan J Z, Cai L, Lin L L and Wang C K 2017 *Phys. Chem. Chem. Phys.* **19** 29872
[28] Zhang K, Zhang Y C, Ma Y Y, Fan J Z, Wang C K and Lin L L 2020 *J. Phys. Chem. A.* **124** 8540
[29] Zhang K, Yang F, Zhang Y C, Ma Y Y, Fan J Z, Fan J, Wang C K and Lin L L 2021 *J. Phys. Chem. Lett.* **12** 1893
[30] Sun L J, Hua W J, Liu Y, Tian G J, Chen M X, Chen M X, Yang F X, Wang S F, Zhang X T, Luo Y and Hu W P 2019 *Angew. Chem. Int. Ed. Engl.* **58** 11311
[31] Zhang Y C, Ma Y Y, Zhang K, Wang C K, Lin L L and Fan J Z 2020 *J. Lumin.* **221** 117046
[32] Liu J, Zhang Y C, Zhang K, Fan J Z, Wang C K and Lin L L 2019 *Org. Electron.* **71** 212
[33] Liu J, Fan J Z, Zhang K, Zhang Y C, Wang C K and Lin L L 2020 *Chin. Phys. B* **29** 088504
[34] Goerigk L, Hansen A, Bauer C, Ehrlich S, Najibi A and Grimme S 2017 *Phys. Chem. Chem. Phys.* **19** 32184
[35] Frisch M J, Trucks G W, Schlegel H B, *et al.* 2016 Gaussian 16 Rev.A.03, Inc., Wallingford, CT
[36] Mccumber D E 1964 *Phys. Rev.* **136** A954
[37] Shuai Z G and Peng Q 2014 *Phys. Rep.* **537** 123
[38] Peng Q, Yi Y P, Shuai Z G and Shao J S 2007 *J. Chem. Phys.* **126** 114302
[39] Shuai Z G 2020 *Chin. J. Chem.* **38** 1223
[40] Lefebvre C, Rubez G, Khartabil H, Boisson J C, Contreras G J and Henon E 2017 *Phys. Chem. Chem. Phys.* **19** 17928
[41] Lu T and Chen F W 2012 *J. Comput .Chem.* **33** 580
[42] Weiner S J, Kollman P A, Case D A, Singh U C, Ghio C, Alagona G, Profeta S Jr and Weiner P 1984 *J. Am. Chem. Soc.* **106** 765
[43] Martin R L 2003 *J. Chem. Phys.* **118** 4775
[44] Xu S, Yang Q Q, Wan Y F, Chen R F, Wang S, Si Y B, Yang B C, Liu D, Zheng C and Huang W 2019 *J. Mater. Chem. C* **7** 9523
[45] Chen R F, Tang Y T, Wan Y F, Chen T, Zheng C, Qi Y Y, Cheng Y F and Huang W 2017 *Sci. Rep.* **7** 6225
[46] Chen L F, Zhang S T, Li H, Chen R F, Jin L, Yuan K, Li H H, Lu P, Yang B and Huang W 2018 *J. Phys. Chem. Lett.* **9** 5240
[47] Liu T T, Chen X J, Zhao J, Wei W C, Mao Z, Wu W, Jiao S B, Liu Y, Yang Z Y and Chi Z G 2021 *Chem. Sci.* **12** 5171
[48] Dalton, A Molecular Electronic Structure Program